COX19 mediates the transduction of a mitochondrial redox signal from SCO1 that regulates ATP7A-mediated cellular copper efflux

Scot C. Leary[a], Paul A. Cobine[b], Tamiko Nishimura[c], Robert M. Verdijk[d], Ronald de Krijger[d], René de Coo[e], Mark A. Tarnopolsky[f], Dennis R. Winge[g], and Eric A. Shoubridge[c]

[a]Department of Biochemistry, University of Saskatchewan, Saskatoon, SK S7N 5E5, Canada; [b]Department of Biological Sciences, Auburn University, Auburn, AL 36849; [c]Montreal Neurological Institute and Department of Human Genetics, McGill University, Montreal, QC H3A 2B4, Canada; Departments of [d]Pathology and [e]Neurology, Erasmus MC University Medical Center, Rotterdam 3000 CA, Netherlands; [f]Department of Pediatrics and Medicine, McMaster University, Hamilton, ON L8N 3Z5, Canada; [g]Departments of Medicine and Biochemistry, University of Utah Health Sciences Center, Salt Lake City, UT 84132

ABSTRACT **SCO1 and SCO2 are metallochaperones whose principal function is to add two copper ions to the catalytic core of cytochrome *c* oxidase (COX). However, affected tissues of *SCO1* and *SCO2* patients exhibit a combined deficiency in COX activity and total copper content, suggesting additional roles for these proteins in the regulation of cellular copper homeostasis. Here we show that both the redox state of the copper-binding cysteines of SCO1 and the abundance of SCO2 correlate with cellular copper content and that these relationships are perturbed by mutations in *SCO1* or *SCO2*, producing a state of apparent copper overload. The copper deficiency in *SCO* patient fibroblasts is rescued by knockdown of ATP7A, a *trans*-Golgi, copper-transporting ATPase that traffics to the plasma membrane during copper overload to promote efflux. To investigate how a signal from SCO1 could be relayed to ATP7A, we examined the abundance and subcellular distribution of several soluble COX assembly factors. We found that COX19 partitions between mitochondria and the cytosol in a copper-dependent manner and that its knockdown partially rescues the copper deficiency in patient cells. These results demonstrate that COX19 is necessary for the transduction of a SCO1-dependent mitochondrial redox signal that regulates ATP7A-mediated cellular copper efflux.**

Monitoring Editor
Thomas D. Fox
Cornell University

Received: Oct 1, 2012
Revised: Dec 17, 2012
Accepted: Jan 17, 2013

INTRODUCTION

Copper is a divalent metal ion that has the ability to rapidly cycle between the Cu(I) and Cu(II) states. This property has been widely exploited across phyla, and copper is used as an essential cofactor in proteins that catalyze or regulate a diverse array of reactions crucial to cellular homeostasis (Kim *et al.*, 2008). However, when it is unbound, copper readily catalyzes the formation of potentially deleterious free radicals. Cells have therefore evolved highly conserved, protein-mediated mechanisms to tightly regulate all aspects of copper handling, including its uptake, efflux, and intracellular trafficking and storage (Kim *et al.*, 2008). These dedicated copper-handling systems ensure that the cytosol is essentially devoid of free copper under normal physiological conditions (Rae *et al.*, 1999).

In mammalian cells, the high-affinity permease CTR1 mediates specific Cu(I) transport across the plasma membrane (Lee *et al.*, 2002). Cu(I) is subsequently transferred to at least two soluble metallochaperones, CCS1 and ATOX1. CCS1 in turn inserts Cu(I) into SOD1 (Lamb *et al.*, 2001), whereas ATOX1 shuttles Cu(I) to the *trans*-Golgi network (TGN), where it is delivered to ATP7A or ATP7B (Banci *et al.*, 2006b). These functionally homologous P-type ATPases then translocate Cu(I) into the lumen of the TGN for its incorporation into secreted cuproenzymes (Petris *et al.*, 2000). However, highly

This article was published online ahead of print in MBoC in Press (http://www.molbiolcell.org/cgi/doi/10.1091/mbc.E12-09-0705) on January 23, 2013.

Address correspondence to: Scot C. Leary (scot.leary@usask.ca).

Abbreviations used: AMS, 4-acetoamido-4′-maleimidylstilbene-2,2′-disulfonic acid; BCS, bathocuproine disulfonic acid; COX, cytochrome *c* oxidase; Cu-His, Cu-histidine; DTT, dithiothreitol; IAM, iodoacetamide; ICP-OES, inductively coupled plasma optical emission spectrometry; ICP-MS, ICP mass spectrometry; IMS, mitochondrial intermembrane space; miRNA, micro RNA; ox, oxidized; PMSF, phenylmethylsulfonyl fluoride; red, reduced; RNAi, RNA interference; SCO, synthesis of cytochrome *c* oxidase; SE, standard error; shRNA, short hairpin RNA; TGN, *trans*-Golgi network.

regulated homeostatic mechanisms also allow for ATP7A and ATP7B to traffic to the cell periphery in response to elevated copper concentrations to efflux copper from the cell (Lutsenko *et al.*, 2007).

Although mitochondria also require copper to metallate two cuproenzymes, cytochrome *c* oxidase (COX) and SOD1, the specific pathway(s) responsible for Cu(I) transport to the organelle are unknown. It is nonetheless clear that the metallation reactions necessary for the assembly of COX and the maturation of SOD1 occur within the mitochondrial intermembrane space (IMS) and require a bioavailable Cu(I) pool that is housed in the mitochondrial matrix (Cobine *et al.*, 2004). The delivery and insertion of copper into COX I and COX II occurs as the holoenzyme is assembled and is facilitated by a surprisingly large number of soluble (COX17, COX19, COX23, PET191, CMC1-3) and integral membrane (COX11, SCO1, SCO2) accessory proteins, termed COX assembly factors (Horn and Barrientos, 2008; Longen *et al.*, 2009; Leary, 2010). Pathogenic mutations have been identified in genes encoding three of these factors: *PET191* (Huigsloot *et al.*, 2011), *SCO1* (Valnot *et al.*, 2000), and *SCO2* (Papadopoulou *et al.*, 1999); however, only those affecting SCO1 and SCO2 function have been investigated in any detail. *SCO1* and *SCO2* patients present with fatal early-onset mitochondrial disease due to a severe, isolated COX deficiency and a profound reduction in total copper content in affected cell types (Leary *et al.*, 2007). Mutations in *SCO2* are associated primarily with neonatal encephalocardiomyopathy, and almost all patients carry at least one *E140K* allele (Papadopoulou *et al.*, 1999; Jaksch *et al.*, 2000, 2001a). In contrast, *SCO1* patients present with more varied clinical symptoms that severely impair liver (Valnot *et al.*, 2000), heart (Stiburek *et al.*, 2009), or brain (Leary, Antonicka, Sasarman, Weraarpachai, Cobine, Pan, Brown, Brown, Majewski, Swartzentruber, Rahman, and Shoubridge, unpublished data) function. Why mutations in ubiquitously expressed paralogues that function in the same biochemical pathway produce such strikingly different, tissue-specific forms of disease is a mystery.

We previously demonstrated that SCO1 and SCO2 fulfill unique but partially overlapping functions in COX assembly and cellular copper homeostasis (Leary *et al.*, 2004, 2007, 2009). The ability of SCO proteins to bind copper is indispensable to these functions and requires the redox-active cysteines of a CxxxC motif and a highly conserved histidine (Balatri *et al.*, 2003; Andruzzi *et al.*, 2005; Horng *et al.*, 2005). It is intriguing that molecular genetic analyses of cultured *SCO* fibroblasts, which phenocopy affected patient tissues, have established that the COX and copper-deficiency phenotypes are dissociable (Leary *et al.*, 2007). The copper deficiency is caused by the inappropriate stimulation of copper efflux from the cell, rather than a defect in its high-affinity uptake, and is rescued to various degrees by overexpressing SCO2 (Leary *et al.*, 2007). Taken together, these observations suggest a model in which SCO2 modifies an aspect of SCO1 function that is crucial to the generation and transduction of a redox signal that regulates copper efflux from the cell. To address this possibility, we used control and patient fibroblast lines to investigate the molecular basis for the SCO-dependent mitochondrial regulation of cellular copper homeostasis.

RESULTS

The redox state of the SCO1 CxxxC motif correlates with total copper content and depends on SCO2 abundance

Cultured *SCO1* and *SCO2* fibroblasts phenocopy affected patient tissues (Leary *et al.*, 2007; Stiburek *et al.*, 2009), making them an excellent model system for interrogating the molecular basis for the SCO-dependent mitochondrial regulation of cellular copper homeostasis. Therefore, to examine a role for redox in modulating the activity of a SCO-dependent mitochondrial signaling pathway, we first analyzed the redox state of the SCO CxxxC motifs in fibroblast lines derived from controls and patients with mutations in one of several COX assembly factors that collectively produce a cellular copper deficiency (Leary *et al.*, 2007). Crude mitochondrial isolates were treated with iodoacetamide (IAM), an agent that irreversibly alkylates cysteine thiols, or 4-acetoamido-4′-maleimidylstilbene-2,2′-disulfonic acid (AMS), an alkylating agent that adds a 0.5-kDa moiety per free thiol group, and electrophoresed under nonreducing conditions to resolve the oxidized and reduced species (Figure 1 and Supplemental Figure S1). In all genetic backgrounds, the cysteines of the CxxxC motif of each SCO protein existed as a mixed population that contained both oxidized disulfides and reduced thiols (Figure 1A and Supplemental Figure S1A; also unpublished data).

Because our previous findings suggested that SCO2 regulates SCO1 function via a thiol-disulfide oxidoreductase activity (Leary *et al.*, 2009), we next expressed the redox state of the SCO1 CxxxC motif as a ratio of reduced to oxidized cysteines and plotted it against total cellular copper content. A significant negative correlation was observed between these two parameters in fibroblast lines derived from controls (Supplemental Figure S2; $r^2 = 0.94$, $p = 0.0029$) and *COX10*, *COX15*, *SCO1*, and *SCO2* patients (Figure 1B and Supplemental Figure S1B). Oxidized cysteines were enriched in copper-replete, control fibroblasts, whereas reduced cysteines were greatly overrepresented in copper-deficient *SCO1* and *SCO2* fibroblast lines. Equivalent results were obtained by treating whole cells or mitochondrial fractions with *N*-ethylmaleimide, an alternative alkylating agent, or with AMS after an initial trichloroacetic acid precipitation step (unpublished data). Consistent with an important role for SCO2 as a thiol-disulfide oxidoreductase, correlation analysis showed a significant relationship between the abundance of SCO2 and the redox state of the SCO1 CxxxC motif (Figure 1C; $r^2 = 0.62$, $p = 0.0059$). Taken together, these data suggest that the ability of SCO2 to regulate the redox state of the SCO1 CxxxC motif is critical to the generation of an appropriate mitochondrial redox signal that impinges upon cellular copper homeostasis.

Compromised redox regulation of the SCO1 CxxxC motif in patient cells signals a state of copper overload that affects ATP7A-dependent copper efflux from the cell

If the disproportionate reduction of the SCO1 CxxxC motif observed in *SCO* patient cells is indeed signaling an apparent state of cellular copper overload, we reasoned that a similar redox signal would be generated in *ATP7A* fibroblasts, whose copper content is significantly increased as a result of the genetic lesion (Supplemental Figure S3B; Horn, 1976; Camakaris *et al.*, 1980). Consistent with this prediction, reduced thiols were enriched more than twofold (2.74 ± 0.51; $p = 0.013$) in the SCO1 CxxxC motif in *ATP7A* fibroblasts as compared with controls (Figure 2A). To further investigate the relationship between the altered redox state of the SCO1 CxxxC motif in *SCO* fibroblasts and cellular copper status, we cultured two control fibroblast lines with the Cu(I)-specific chelator bathocuproine disulfonic acid (BCS) to pharmacologically induce a cellular copper deficiency (~30% of parental). Oxidized cysteines were enriched roughly threefold (3.59 ± 0.90, $p = 0.003$) in the SCO1 CxxxC motif of BCS-treated control fibroblasts relative to parental cells (Figure 2B), an effect that was observed in the absence of significant changes in residual COX activity (Dodani *et al.*, 2011) or SCO protein abundance (Supplemental Figure S4). Treatment of patient fibroblasts with BCS also caused significant reductions in total cellular copper content (*SCO2* and *ATP7A*; 19 and 62% of parental, respectively); however, oxidation of the cysteines in the SCO1 CxxxC motif

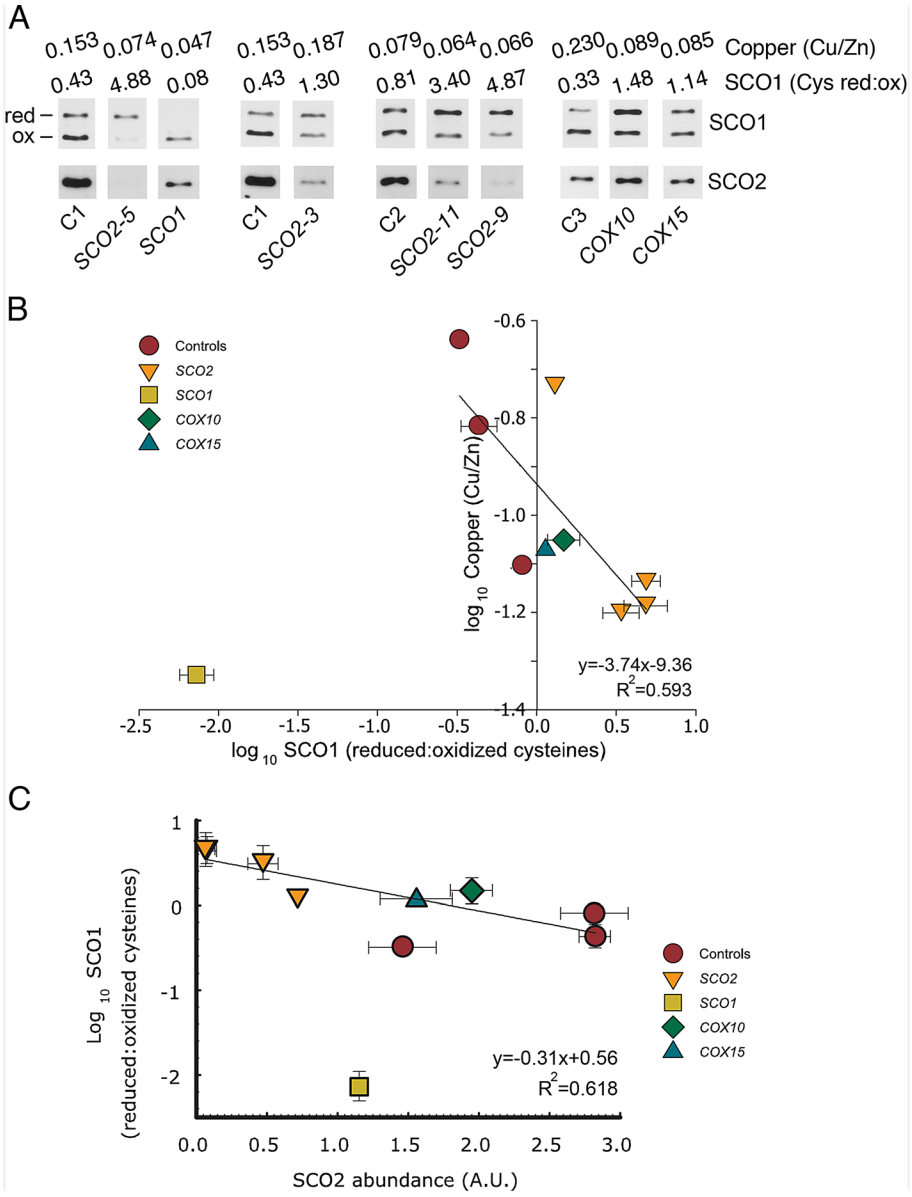

FIGURE 1: The redox state of the SCO1 CxxxC motif is significantly correlated with cellular copper levels and SCO2 abundance in cultured fibroblasts. (A) Isolated mitochondria (2 mg/ml) from control ($n = 3$), *SCO1*, *SCO2* (*SCO2-3*, *SCO2-5*, *SCO2-9*, *SCO2-11*), *COX10*, and *COX15* fibroblasts were incubated in iodoacetamide (I) for 1 h at room temperature, denatured in sample loading buffer in the absence of reductant, and electrophoresed (25 µg/lane) under nonreducing conditions (Leary *et al.*, 2009). The redox state of the SCO1 CxxxC motifs was then detected by immunoblotting with a specific polyclonal antibody (Leary *et al.*, 2004). ox, oxidized disulfides; red, iodoacetamide-modified, reduced thiols. The relative abundance of both redox species was quantified by densitometric analysis of multiple exposures within the linear range of the film ($n =$ 3–4), using ImageQuant software (Leary *et al.*, 2009). The redox state of the SCO1 CxxxC motif was then expressed as the mean ratio of reduced thiols to oxidized disulfides (i.e., Cys red:ox). For SCO2, the electrophoretic mobility of each redox species is identical (Leary *et al.*, 2009), and the immunoreactive band therefore represents total protein abundance. The copper content of fibroblast lines was also measured by ICP-OES and normalized to total cellular zinc. Mutations specific to each patient background are provided in *Materials and Methods*. (B) The mean ratio of reduced thiols to oxidized disulfides of SCO1 ± SE plotted as a function of total cellular copper content after each parameter had been log transformed. Statistical analysis yielded a high Pearson's r (–0.78) and revealed a significant correlation between these two parameters ($p = 0.0062$). (C) The mean abundance of SCO2 ± SE quantified by densitometry as described in A and plotted in arbitrary units (A.U.) against the log transformation of the mean ratio of reduced thiols to oxidized disulfides of SCO1 ± SE. Statistical analysis calculated a high Pearson's r (–0.79) and detected a significant correlation between these two parameters ($p = 0.0059$). For both B and C the data point for *SCO1* fibroblasts was omitted from the regression analyses.

was markedly attenuated in both patient backgrounds (*SCO2* and *ATP7A*; 1.47 ± 0.07 and 0.87 ± 0.05, respectively; Figure 2B). These data suggest that the inability to appropriately regulate the redox state of the SCO1 CxxxC motif in *SCO* patient cells signals a copper overload state that ultimately leads to a cellular copper deficiency.

The copper overload phenotype in *ATP7A* fibroblasts (Supplemental Figure S3; Horn, 1976; Camakaris *et al.*, 1980) suggests that trafficking of ATP7A between the TGN and plasma membrane represents the dominant mechanism for effluxing copper in this cell type. To investigate the role of ATP7A in copper efflux in *SCO* patient cells, we first used a short hairpin RNA (shRNA) to stably knock down SCO1 in two *ATP7A* fibroblast lines. We then overexpressed SCO1 P174L in those clones that exhibited the most marked SCO1 knockdown (Figure 2C). Although this combined expression strategy produces a severe cellular copper-deficiency phenotype in control fibroblasts (Leary *et al.*, 2007), it did not significantly affect the copper content of clones derived from *ATP7A* fibroblasts (Figure 2D), arguing that ATP7A is required to effect cellular copper efflux in response to the aberrant redox signaling through SCO1 P174L. To further test this hypothesis, we used two different RNA interference (RNAi) duplexes to transiently knock down ATP7A in control, *SCO1*, and *SCO2* fibroblasts. Treatment for 6 d with either RNAi duplex resulted in the lack of immunodetectable ATP7A in all cell lines (Figure 2E) and a disproportionate increase in copper levels in *SCO* fibroblasts relative to control cells (*SCO1* and *SCO2*; 186 and 147% of control, respectively; Figure 2F). As expected, the copper content of *ATP7A* fibroblasts was unaffected by treatment with either RNAi duplex.

COX19 partitions between mitochondria and the cytosol and is critical to the transduction of an SCO1-dependent redox signal

Because SCO1 and SCO2 are integral membrane proteins, the transduction of a SCO1-dependent redox signal to extramitochondrial compartments likely requires an intermediary signaling molecule(s). The small, soluble COX assembly factors are attractive candidates in this respect because they contain highly conserved twin Cx_9C motifs that may provide for direct redox monitoring of the functional status of SCO1 (Leary, 2010) and because there is some evidence to suggest that several of the yeast orthologues are dually localized to the IMS and the cytosol (Glerum *et al.*, 1996; Nobrega *et al.*, 2002; Barros *et al.*, 2004). To begin to investigate

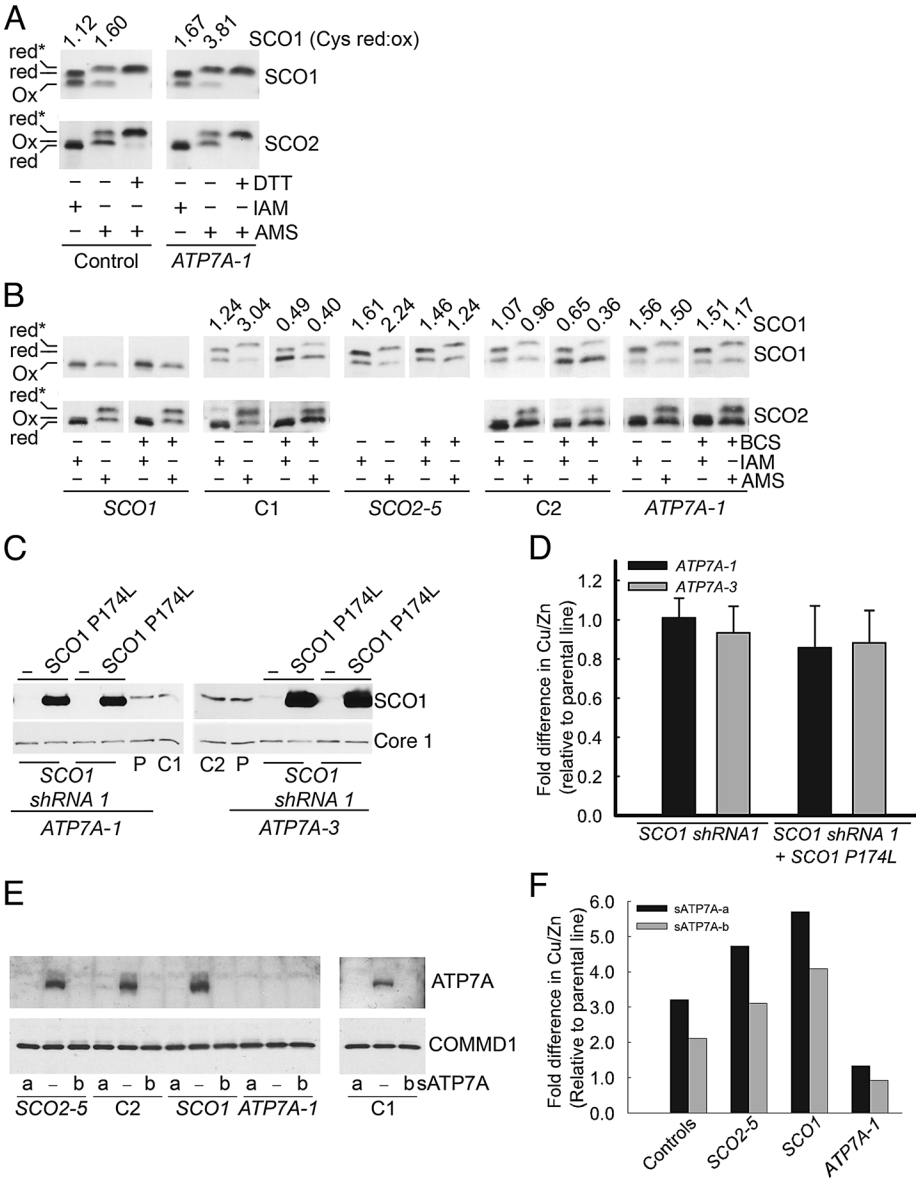

this possibility, we analyzed the steady-state levels of COX17, COX19, COX23, and PET191 in control and *SCO1* and *SCO2* patient cells (Figure 3). The steady-state levels of COX19 and COX23 were reduced, whereas those of COX17 and PET191 were increased in *SCO* patient cells (Figure 3, A–C). To test whether the altered steady-state levels of these proteins in *SCO* patient cells were simply a consequence of the isolated COX deficiency, we measured their abundance in control fibroblasts cultured in the absence or presence of BCS at a concentration that pharmacologically depleted cellular copper content without significantly affecting COX activity (Dodani *et al.*, 2011). The expression profile of all four proteins generally phenocopied that observed in *SCO* patient cells, suggesting that their abundance is regulated by cellular copper status (Figures 3D and 4A; also unpublished data).

Although short-term treatment of control fibroblast lines with BCS consistently produced an increase in the abundance of PET191 at the whole-cell level, we did not always observe a corresponding reduction in the steady-state levels of COX19 (e.g., Figure 3D vs. Figure 4A; also unpublished data). Subsequent immunoblot analysis of whole-cell extracts derived from three *ATP7A* fibroblast lines (Figure 3E) and several affected *SCO* patient tissues (Supplemental Figure S5) similarly revealed that the only consistent change in the expression of either of these COX assembly factors was the increased abundance of PET191. These observations led us to postulate that an altered subcellular distribution of COX19 precedes the stabilization of PET191 and may

FIGURE 2: The impaired redox regulation of the SCO1 CxxxC motif in *SCO* fibroblasts signals a state of apparent copper overload that affects ATP7A-dependent cellular copper efflux. (A) Isolated mitochondria (2 mg/ml) from control and *ATP7A-1* fibroblasts were incubated in the presence or absence of DTT, treated with IAM or AMS, and then denatured and electrophoresed (25 μg/lane) under nonreducing conditions (Leary *et al.*, 2009). The redox state of the SCO CxxxC motifs was detected by immunoblotting with specific polyclonal antisera raised against each protein. ox, oxidized disulfides; red, iodoacetamide-modified, reduced thiols; red*, the AMS-induced shift in the electrophoretic mobility of reduced thiols, which is caused by the addition of a 0.5-kDa moiety per thiol group. (B) Control (C1, C2), *SCO1*, *SCO2-5*, and *ATP7A-1* fibroblasts were cultured for 36 h in the absence or presence of 100 μM BCS. Mitochondria were then isolated, treated with IAM or AMS, electrophoresed, and immunoblotted as described in A. For A and B, the relative abundance of both redox species of SCO1 was quantified by densitometric analysis of multiple exposures within the linear range of the film ($n = 3–4$), using ImageQuant software (Leary *et al.*, 2009). The redox state of each CxxxC motif in IAM- and AMS-treated samples was then expressed as the mean ratio of reduced thiols to oxidized disulfides (i.e., Cys red:ox). For statistical analyses, the Cys red:ox of each IAM- and AMS-treated sample at a given exposure was averaged, and a two-tailed, Student's *t* test was used to detect significant differences in the redox state of the SCO1 CxxxC motif between (A) control and *ATP7A-1* fibroblasts and (B) untreated and BCS-treated fibroblasts, with the associated *p* values provided in *Results*. (C, D) Two *ATP7A* fibroblast lines were stably transduced with an shRNA (*SCO1 shRNA 1*) that targets the 3′ untranslated region of *SCO1* mRNA (Leary *et al.*, 2007) and plated at clonal density, and SCO1 abundance in individual clones (–) was compared with parental (P) and control (C1, C2) lines. Select clones (*ATP7A-1*, $n = 5$; *ATP7A-3*, $n = 3$) were then retrovirally transduced to overexpress SCO1 P174L, and the phenotypic effects on cellular copper content were quantified by ICP-OES. A one-way analysis of variance (ANOVA) failed to detect a significant effect (i.e., $p < 0.05$) of manipulating the expression of SCO1 variants on total cellular copper content in either ATP7A patient background. (E, F) Control (C1, C2), *SCO1*, *SCO2-5*, and *ATP7A-1* fibroblasts were cultured in the absence (–) or presence of one of two different Stealth RNAi duplexes (a, b; see Supplemental Table S1) to knock down ATP7A abundance. After 6 d, cells were harvested and their copper content quantified by ICP-MS. Whole-cell extracts (10 μg/lane) were also prepared and fractionated on a 5–20% gradient gel under denaturing conditions (Leary *et al.*, 2007), and the membrane was blotted with a specific polyclonal antiserum to detect ATP7A. COMMD1 served as an internal loading control.

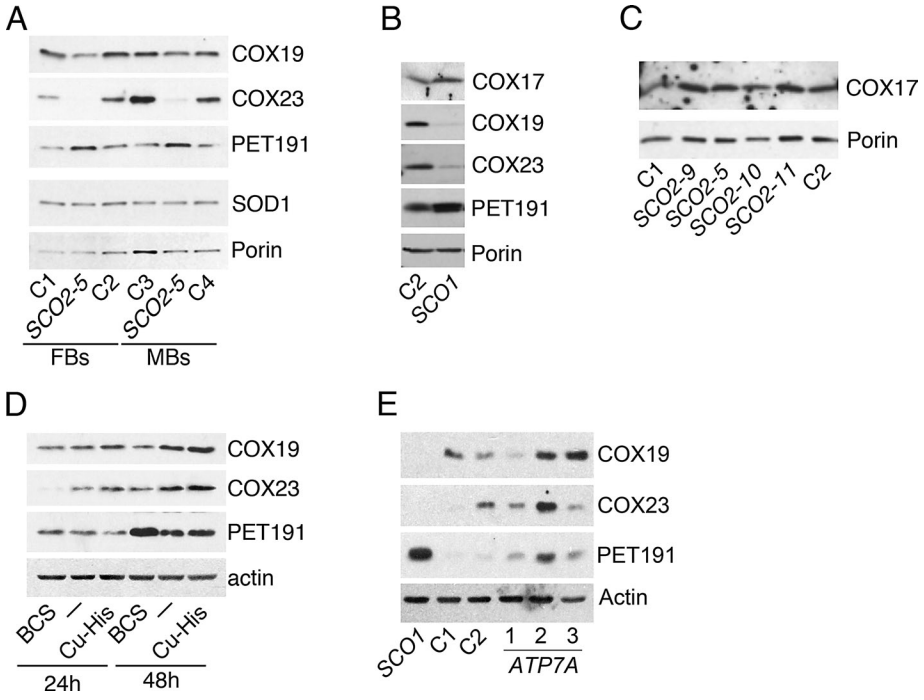

FIGURE 3: The abundance of several soluble twin Cx_9C motif–containing COX assembly factors is sensitive to cellular copper status. (A, B) Whole-cell extracts (15 µg/lane) from control (C1–C4), *SCO1*, and *SCO2-5* fibroblasts (FBs) or myoblasts (MBs) and (C) mitochondrial extracts (10 µg/lane) from control (C1, C2) and *SCO2* ($n = 4$) fibroblasts were electrophoresed by SDS–PAGE on 5–20% gradient gels under denaturing conditions. Membranes were decorated with polyclonal antisera to detect COX17, COX19, COX23, and PET191. Porin and SOD1 served as internal loading controls. (D) Whole-cell extracts (15 µg/lane) from a control fibroblast line cultured for 24 or 48 h in basal media or media supplemented with 100 µM of the Cu(I) chelator BCS or Cu-His were fractionated by SDS–PAGE on 5–20% gradient gels under denaturing conditions. Membranes were then decorated with the polyclonal antisera to detect COX19, COX23, and PET191. Actin served as an internal loading control. (E) Whole-cell extracts (15 µg/lane) from two control (C1, C2) and three *ATP7A* fibroblast lines (*ATP7A-1*, *-2*, and *-3*) were fractionated by SDS–PAGE on 5–20% gradient gels under denaturing conditions, and membranes were blotted with polyclonal antisera to detect COX19, COX23, and PET191. Actin served as an internal loading control. An equivalent amount of whole-cell extract isolated from *SCO1* fibroblasts was included in these analyses as a positive control.

be critical to the transduction of a redox signal that regulates cellular copper homeostasis. To directly test this hypothesis, we first analyzed the relative abundance of COX19, COX23, and PET191 in whole-cell, mitochondrial (Mt) and highly purified cytosolic (soluble [S], pellet [P]) fractions isolated from control, *SCO1*, and *ATP7A* fibroblasts (Figure 4). Control fibroblasts grown in media supplemented with BCS or Cu-histidine (Cu-His) were included in these analyses as a pharmacological complement to the two patient backgrounds. Of the three COX assembly factors that were investigated, only COX19 localized to both the mitochondrial and cytosolic fractions (Figure 4B). Of importance, COX19 was enriched not only in the cytosolic fraction of *ATP7A* fibroblasts and control fibroblasts cultured with Cu-His, but also in *SCO1* fibroblasts, in spite of their severe cellular copper deficiency.

If the relative subcellular distribution of COX19 is indeed critical to the transduction of a mitochondrial redox signal that regulates cellular copper efflux, we reasoned that knocking it down in control fibroblasts would perturb copper homeostasis. We therefore quantified total copper content in control fibroblast lines in which COX19 had been stably knocked down using a specific micro RNA (miRNA) or D3, the most effective of the COX19 shRNAs that were screened (Figure 5, A–C). Stable knockdown of COX19 with either RNAi significantly reduced cellular copper levels relative to the parental line, whereas total copper content was unaffected by the stable knockdown of PET191 (Figure 5, B and C). In contrast, only the knockdown of PET191 resulted in a significant reduction in COX activity in control and *SCO* fibroblasts (Supplemental Figure S6). To further investigate the role of COX19 in the regulation of cellular copper levels, we measured the effect of knocking it down on cellular copper levels in several patient backgrounds. Knockdown of COX19 in *SCO1*, *SCO2*, and *COX15* fibroblasts increased cellular copper levels by ~30–60% but did not alter the copper content of *ATP7A* fibroblasts (Figure 5D). Consistent with a role for COX19 in transducing a SCO1-dependent signal, its steady-state levels were further reduced after stable knockdown of SCO1 P174L (Figure 5E), which we previously showed partially rescues the copper-deficiency phenotype in *SCO1* fibroblasts (Leary *et al.*, 2007).

DISCUSSION

This study demonstrates that COX19 is necessary for the transduction of a SCO1-dependent mitochondrial redox signal that regulates ATP7A-mediated copper efflux from the cell. Several lines of evidence support this conclusion. First, the copper content of fibroblasts correlates with the redox state of the SCO1 CxxxC motif and the steady-state level of SCO2. Second, mutations in *SCO1* or *SCO2* alter the redox state of the SCO1 CxxxC motif and cause a cellular copper deficiency that can be rescued by silencing ATP7A expression. Third, COX19 distributes between the IMS and the cytosol in a copper-dependent manner that is perturbed in *SCO* patient cells. Finally, stable knockdown of COX19 differentially affects cellular copper homeostasis in control and *SCO* fibroblasts but does not alter the total copper content of *ATP7A* fibroblasts.

SCO1 and SCO2 require their CxxxC motifs for COX assembly and the regulation of cellular copper homeostasis (Leary *et al.*, 2004, 2007; Horng *et al.*, 2005; Banci *et al.*, 2006a; Stiburek *et al.*, 2009). SCO2 appears to act upstream of SCO1 in both of these pathways (Leary *et al.*, 2007, 2009). These observations suggested that modulation of the redox state of the SCO1 CxxxC motif by SCO2 could generate a signal controlling cellular copper efflux. Consistent with this idea, we detected a robust correlation between total copper content and the redox state of the SCO1 CxxxC motif in control and patient fibroblasts. Correlation analysis also established that the redox state of the SCO1 CxxxC motif is directly proportional to SCO2 abundance in this cell type, supporting a role for SCO2 in regulating the functional status of SCO1 via a thiol-disulfide oxidoreductase activity (Leary *et al.*, 2009).

Pathogenic mutations in *SCO1* and *SCO2* would be predicted to impair the mitochondrial signaling pathway regulating cellular copper homeostasis because they compromise SCO protein function by altering their redox properties (Williams *et al.*, 2005; Cobine *et al.*, 2006; Banci *et al.*, 2007). Indeed, our analyses of cultured cells

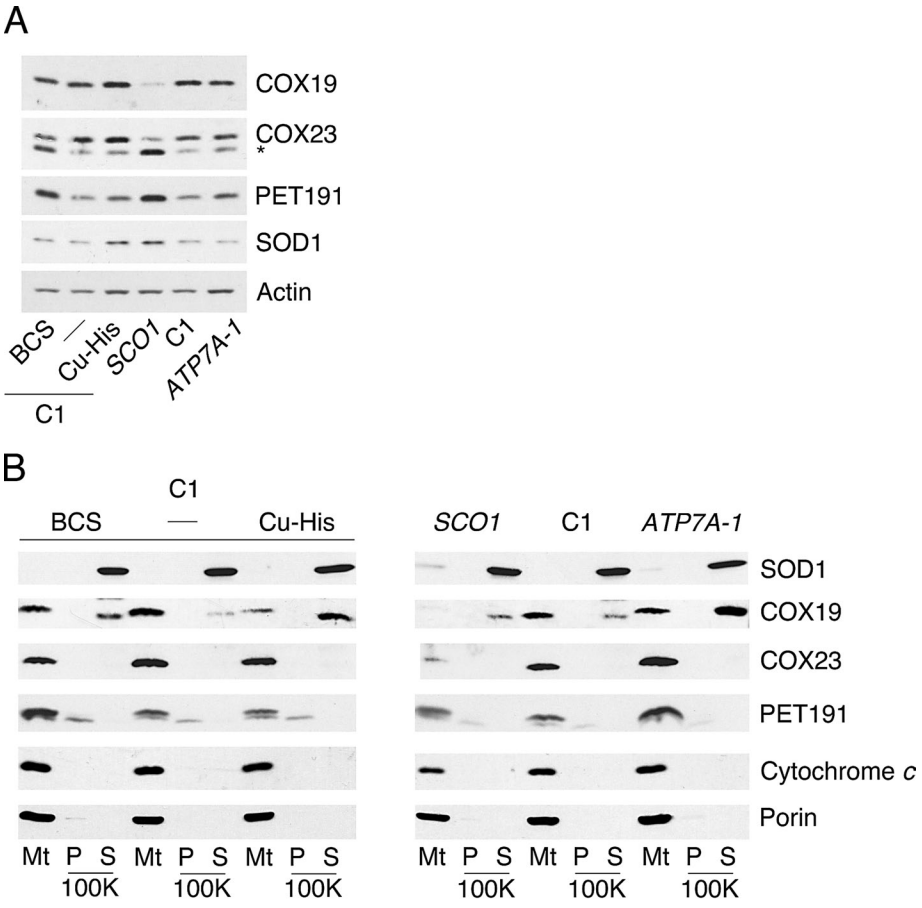

FIGURE 4: COX19 partitions between mitochondria and the cytosol in a copper-dependent manner. (A) Whole-cell extracts were prepared from *SCO1* and *ATP7A-1* fibroblasts, as well as a single control fibroblast line (C1) cultured for 24 h in basal media (–), or media supplemented with 100 μM BCS or Cu-His. Denatured extracts (10 μg/lane) were electrophoresed by SDS–PAGE on 5–20% gradient gels under denaturing conditions and membranes decorated with polyclonal antisera to detect COX19, COX23, and PET191. The asterisk denotes residual PET191 immunoreactivity detected upon blotting for COX23. (B) A crude mitochondrial fraction (Mt) was isolated by differential centrifugation from all of the cells described and analyzed in A. The resultant supernatant was subsequently spun for 1 h at 100,000 × *g* at 4°C to isolate the soluble cytosolic fraction (S) from the insoluble fraction (P), which comprises a minor amount of mitochondria, as well as endoplasmic reticulum, Golgi, and microsomes. The abundance of COX19, COX23, and PET191 in all three fractions (10 μg/lane) was then detected by Western blotting. Exclusive localization of porin and the IMS protein cytochrome *c* to the Mt fraction argue that the isolated organelles were intact. SOD1 served as a cytosolic marker.

demonstrated that the SCO1 CxxxC motif is disproportionately reduced in copper-deficient *SCO1* and *SCO2* fibroblasts. The one notable exception is the CxxxC motif of SCO1 P174L, which is almost entirely oxidized (Leary *et al.*, 2009). However, the *P174L* allele severely attenuates the ability of mutant SCO1 to interact with its Cu(I) donor COX17 (Cobine *et al.*, 2006; Banci *et al.*, 2007), and it is unique among the pathogenic alleles we have investigated thus far in that it prevents SCO2 overexpression from fully rescuing the copper-deficiency phenotype (Leary *et al.*, 2007). We therefore favor the idea that SCO1 P174L structurally resembles the SCO1 conformer found in other copper-deficient patient fibroblasts and similarly missignals a state of cellular copper overload (Leary *et al.*, 2007). Although we do not yet know whether this conformer is apo- or copper-loaded SCO1, two additional observations corroborate a causal role for the altered redox state of its CxxxC motif in generating an aberrant signal. First, a disproportionate reduction of the SCO1 CxxxC motif is observed in *ATP7A* fibroblasts, which, as opposed to *SCO* patient cells, have significantly higher copper levels than control fibroblasts (Horn, 1976; Camakaris *et al.*, 1980). Second, the cysteinyl sulfurs of the motif are shifted toward an oxidized state in control fibroblasts treated with BCS to chemically mimic the copper deficiency in *SCO* patient cells.

Our data support a model in which inappropriate redox regulation of the SCO1 CxxxC motif potentiates the trafficking of ATP7A to the plasma membrane, where it catalyzes copper efflux from the cell. Transient knockdown of ATP7A results in a disproportionate increase in cellular copper levels in *SCO* fibroblasts relative to control cells. Of importance, the residual copper content of *ATP7A* fibroblasts was unaffected by either Stealth RNAi duplex, arguing that functional complementation of the copper deficiency in *SCO* patient cells was directly attributable to ATP7A knockdown rather than an off-target effect. Consistent with these observations, cellular copper levels were also unchanged in several *ATP7A* fibroblast clones in which endogenous SCO1 had been stably knocked down and SCO1 P174L subsequently overexpressed, a strategy that produces a cellular copper deficiency in control fibroblasts (Leary *et al.*, 2007). Taken together, these findings argue that ATP7A is required to efflux copper from the cell in response to SCO-dependent mitochondrial redox signaling. It is unclear why, unlike other experimental systems (Petris and Mercer, 1999; Hamza *et al.*, 2003; Kim *et al.*, 2010), the elevated rate of copper efflux in *SCO* fibroblasts is not accompanied by an increase in ATP7A abundance or its marked redistribution from the TGN to the plasma membrane (Leary *et al.*, 2007). However, kinetic labeling studies with ^{64}Cu demonstrated that only a small percentage of the total pool of ATP7A is required to effect rapid changes in the rate of copper efflux from the cell (Pase *et al.*, 2004). Our working hypothesis therefore remains that in patient cells, SCO1 generates an inappropriate redox signal that stimulates the trafficking of a minor, but physiologically significant, fraction of the total cellular pool of ATP7A to the plasma membrane.

The transduction of a SCO-dependent redox signal from mitochondria to ATP7A requires COX19. Mutations in either *SCO* gene alter its abundance, as well as that of COX17, COX23, and PET191, three other members of a large family of small, soluble COX assembly factors that localize predominantly to the IMS and contain highly conserved twin Cx_9C motifs (Glerum *et al.*, 1996; Nobrega *et al.*, 2002; Barros *et al.*, 2004; Longen *et al.*, 2009). The altered expression profile observed for these proteins in cultured *SCO* patient cells is largely recapitulated in BCS-treated, control fibroblasts, arguing that their steady-state levels are regulated by cellular copper status. However, COX19 is unique among the family members we investigated in that it partitions between the IMS and the cytosol in a copper-dependent manner. The cytosol is

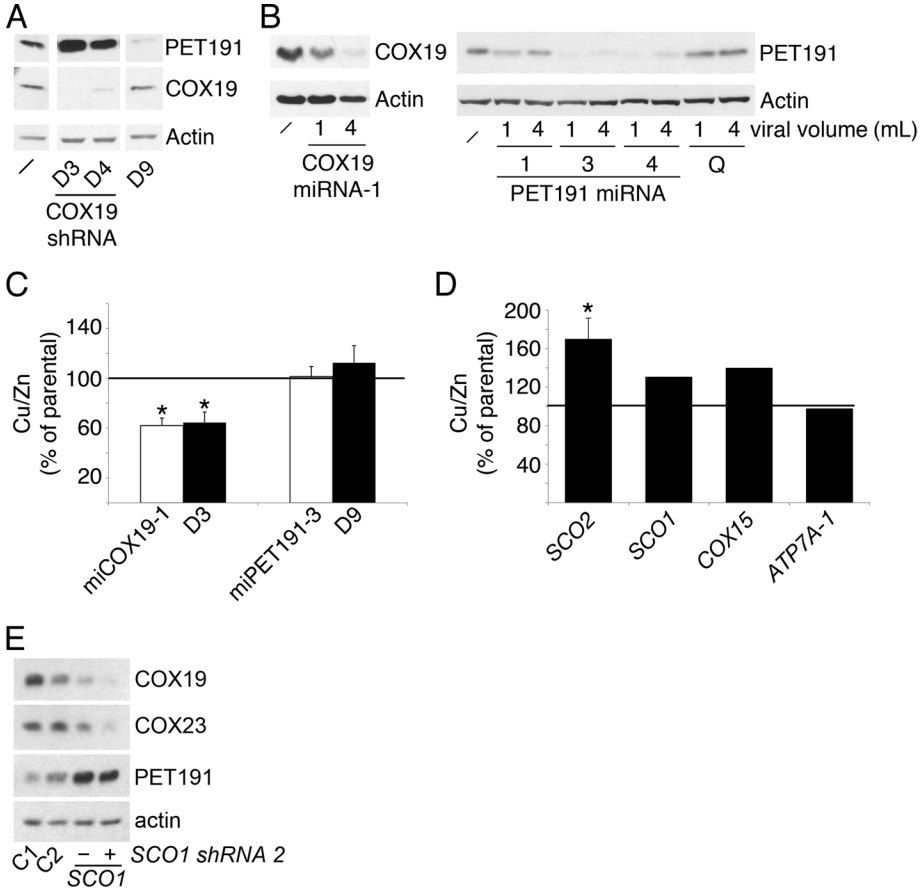

FIGURE 5: COX19 is critical to the transduction of a SCO1-dependent mitochondrial redox signal that regulates cellular copper homeostasis. (A, B) The abundance of COX19 or PET191 was stably knocked down in control fibroblasts using either a specific shRNA or miRNA (see Supplemental Table S1 for further details) and compared with the parental line (–). Whole-cell extracts were prepared and electrophoresed (10 μg/lane) under denaturing conditions, and membranes were blotted with polyclonal antisera to detect each protein. Actin served as an internal loading control. D3 and D4 are shRNAs targeted to *COX19* mRNA, whereas D9 is an shRNA specific to *PET191* mRNA. For the miRNA experiments, Q denotes a scrambled, control sequence (see Supplemental Table S1 for further details). (C, D) Quantification of the phenotypic effects of stably knocking down COX19 or PET191 on total cellular copper levels in control, *SCO1*, *SCO2* (*SCO2-3*, *SCO2-5*, *SCO2-9*), *COX15*, and *ATP7A-1* fibroblasts. Data are presented as mean total cellular copper content ± SE. Asterisk denotes a statistically significant difference ($p < 0.0001$) in total copper content between parental and knockdown cells for control (COX19-1 miRNA, $n = 3$; D3 COX19 shRNA, $n = 5$) and *SCO2* (D3 COX19 shRNA, $n = 3$) fibroblasts, detected by a one-way ANOVA and Tukey's HSD post hoc test. Equivalent statistical analyses were not performed for remaining patient fibroblast lines because the data represent single point measurements. (E) Whole-cell extracts were prepared from control (C1, C2) and *SCO1* fibroblasts alone and from *SCO1* fibroblasts stably expressing an shRNA (*SCO1 shRNA 2*) that targets the 3′ untranslated region of *SCO1* mRNA to knock down the abundance of SCO1 P174L (Leary *et al.*, 2007). Denatured extracts (10 μg/lane) were fractionated by SDS–PAGE on 15% SDS–PAGE gels under denaturing conditions and membranes decorated with polyclonal antisera to detect COX19, COX23, and PET191. Actin served as an internal loading control.

relatively enriched for COX19 when intracellular copper concentrations are elevated (e.g., control cells + Cu-His, *ATP7A* fibroblasts) and, surprisingly, in copper-deficient *SCO1* fibroblasts. These observations suggested to us that an increase in the pool of COX19 localized to the cytosol is critical for signaling a state of apparent copper overload. Consistent with this idea, stable knockdown of COX19 partially complemented the copper-deficiency phenotype in *COX15*, *SCO1*, and *SCO2* fibroblasts. However, the copper deficiency in control fibroblasts induced by knockdown of COX19 emphasizes that its presence within the IMS is also essential for the transduction of appropriate SCO-dependent redox signals outside mitochondria. The lack of a phenotypic effect of reduced COX19 expression on the residual copper content of *ATP7A* fibroblasts is in marked contrast with our observations in other genetic backgrounds and further corroborates a role for ATP7A as the effector in this signaling pathway.

Of interest, the steady-state levels of COX19 are in the control range in *SCO2* hearts, despite the fact they are copper deficient and exhibit a marked increase in the abundance of PET191. Evidence from our cell culture system argues that PET191 is exclusively localized to mitochondria and that its abundance within the IMS only increases when COX19 preferentially localizes to the cytosol. We therefore believe that the steady-state levels of PET191 are a reliable, surrogate measure of the relative enrichment for COX19 in the cytosol. Consistent with a primary role for COX19 in the cytosolic transduction of a mitochondrial redox signal, its knockdown affects only residual COX activity in *SCO1* fibroblasts, further exacerbating the observed COX deficiency. Although this provides genetic evidence of a direct interaction between COX19 and SCO1, it also suggests that this interaction is not normally required for holoenzyme assembly because it can be detected only when COX19 knockdown is paired with the expression of a severely crippled *SCO1* allele (Cobine *et al.*, 2006; Banci *et al.*, 2007). However, it is unlikely that COX19 acts alone to monitor the functional status of SCO1, given the pleiotropic effects of altered cellular copper status on the abundance of several soluble, IMS-localized COX assembly factors. Detailed investigations are ongoing of how the functional interrelationships between members of this protein family contribute to the transduction of an SCO1-dependent redox signal from the mitochondrion to ATP7A to regulate cellular copper homeostasis.

MATERIALS AND METHODS

Tissue culture and cell lines

Primary fibroblasts from control, *SCO1* (R149X/P174L; Valnot *et al.*, 2000), *SCO1-2* (V93X/M294V; Leary *et al.*, unpublished data), *SCO2-6* and *SCO2-11* (E140K/E140K; Jaksch *et al.*, 2001a), *SCO2-3* (R171W/E140K) and *SCO2-5* (R90X/E140K; Jaksch *et al.*, 2000), *SCO2-9* and *SCO2-10* (R90X/E140K; this study), *COX10* (Antonicka *et al.*, 2003a), *COX15* (Antonicka *et al.*, 2003b), and *ATP7A-1*, *-2*, and *-3* patients were immortalized as previously described (Leary *et al.*, 2004). Phoenix amphotropic packaging cells for the helper-free production of retrovirus were obtained from G. Nolan (Stanford University, Stanford, CA). All cell lines were grown in high-glucose DMEM supplemented with 10% fetal bovine serum at 37°C in an atmosphere of 5% CO_2 and tested to ensure that they

were *Mycoplasma*-free (MycoAlert; Cambrex Bio Science, Verviers, Belgium) before harvesting.

Retroviruses containing the SCO1 P174L cDNA or the shRNAs targeting the untranslated regions of *SCO1* mRNA (Leary *et al*., 2007) were produced as described in detail elsewhere (Pear *et al*., 1993). The resultant retroviruses were then used to transduce fibroblasts proliferating at 40–60% confluency, and stable overexpression cell lines were selected in media containing hygromycin or puromycin alone or a combination of both drugs (Leary *et al*., 2004).

RNA interference

For transient knockdown experiments, Stealth RNAi duplexes against *COX19*, *COX23*, *PET191*, and *ATP7A* mRNA (Invitrogen, Carlsbad, CA) were used (see Supplemental Table S1). Stealth RNAi duplexes were transiently transfected into immortalized fibroblasts at 50% confluency using Lipofectamine RNAiMAX (Invitrogen), according to the manufacturer's specifications. Maximal knockdown was achieved by transfection of cells with each Stealth RNAi duplex on days 1 and 3 for their eventual harvest on day 6.

Stable knockdown of COX19 or PET191 was achieved by lentiviral transduction of subconfluent fibroblasts with vectors containing either a shRNA or miRNA against each mRNA (see Supplemental Table S1). Lentiviral vectors containing COX19 and PET191 MISSION shRNAs were purchased from Sigma-Aldrich (St. Louis, MO), and virus was transiently produced using a protocol outlined in detail by the RNAi consortium (Moffat *et al*., 2006). Expression plasmids for miRNAs were constructed in a multistep process that first involved designing oligonucleotide pairs for cloning into pcDNA6.2/GW-EmGFP-miR using the BLOCK-iT Pol II miR RNAi Expression Vector Kit (Invitrogen). Sequence-verified clones were then used as PCR templates to amply the miRNA cassettes using the primers 5′-GCGCAGATCTACCGGTCGCCACCATGGTGAGCAAGGGCGAGGAGC-3′ and 5′-GCGCCTCGAGTGCGGCCGGATCTGGGCCATTTGTTCCATGTGAGTGC-3′. PCR products were digested with *Bgl*II and *Xho*I, ligated into *Bam*HI/*Sal*I-digested pRRLsinPPT-eGFP, and transformed into TOP10 *Escherichia coli*. Sequence-verified miRNA expression plasmids were subsequently used for lentiviral production in 293T cells. Briefly, 293T cells were cotransfected with miRNA-containing pRRLsinPPT-eGFP, pMDLg/RRE, MD2.g, and pRSV-Rev using a standard $CaCl_2$ transfection method. Virus-containing supernatant was collected three times over 48 h and concentrated by ultracentrifugation. Lentiviral transduction of fibroblasts was done in the presence of 4 μg/ml polybrene (Sigma-Aldrich). Stable shRNA-expressing fibroblast cultures were selected in puromycin (Leary *et al*., 2007), and fibroblasts stably expressing individual miRNAs were isolated by fluorescence-activated cell sorting based on green fluorescent protein fluorescence.

Subcellular fractionation

Whole cells were homogenized on ice in STE buffer (250 mM sucrose, 10 mM Tris-HCl, pH 7.4, and 1 mM EDTA) supplemented with a 1× protease inhibitor cocktail (Roche, Indianapolis, IN) and 0.5 mM phenylmethylsulfonyl fluoride (PMSF; Sigma-Aldrich) and centrifuged twice at 4°C for 10 min at 600 × *g* to obtain a postnuclear supernatant. A crude mitochondrial fraction was then obtained by centrifugation at 4°C for 10 min at 8000 × *g*. The supernatant from the postmitochondrial fraction was recentrifuged at 4°C for 1 h at 100,000 × *g* using a TLA100.1 rotor and a Beckman bench-top ultracentrifuge. The resultant high-speed supernatant and pellet were recovered. Both pellets in this purification scheme were washed once with 10 volumes of fresh isolation buffer to deplete residual contaminants, and all three fractions were then analyzed by Western blotting.

Reducing and nonreducing PAGE analyses

Extracts were prepared from whole cells, digitonized mitoplasts, and various subcellular fractions using a buffer containing 0.25% Triton X-100 (Leary *et al*., 2007) or 1.5% lauryl maltoside (Leary *et al*., 2004) and electrophoresed by SDS–PAGE as previously described (Leary *et al*., 2004, 2007). For nonreducing SDS–PAGE experiments, isolated mitochondria (2 mg/ml) were resuspended in a standard mitochondrial import buffer (Steenaart and Shore, 1997) supplemented with 0.1 mg/ml bovine serum albumin, 0.5 mM PMSF, and a 1× protease inhibitor cocktail in the presence or absence of 50 mM dithiothreitol (DTT; EM Biosciences, San Diego, CA) and incubated for 20 min at room temperature. Mitochondria were then pelleted by centrifugation at 8000 × *g* for 5 min at 4°C and lysed in a buffer containing either 50 mM iodoacetamide (Sigma-Aldrich) or 25 mM 4-acetoamido-4′-maleimidylstilbene-2,2′-disulfonic acid (Invitrogen; Leary *et al*., 2009). After a 1 h incubation at room temperature, an equal volume of 2× sample loading buffer (Bio-Rad, Hercules, CA) minus reductant was added, and samples were boiled for 5 min and loaded onto 15% Tris-HCl Criterion gels (Bio-Rad) that had been prerun at 120 V for 30 min. Both reducing and nonreducing SDS–PAGE gels were transferred to nitrocellulose membranes under semidry conditions and were decorated with monoclonal antibodies raised against porin (Calbiochem, La Jolla, CA), actin (Sigma-Aldrich), cytochrome *c*, and SDH70 (Molecular Probes, Eugene, OR) or polyclonal antisera raised against SOD1 and SOD2 (Stressgen, San Diego, CA), COX17 (Leary *et al*., 2007), SCO1 (Leary *et al*., 2004), SCO2 (Jaksch *et al*., 2001b), ATP7A (kind gift of B. A. Eipper, University of Connecticut, Farmington, CT), and COMMD1 (kind gift of C. S. Duckett, University of Michigan, Ann Arbor, MI). Polyclonal antisera were raised against histidine-tagged, full-length recombinant COX19, COX23, and PET191 in rabbits and then affinity purified (Pierce, Rockford, IL) as described elsewhere for COX17 (Leary *et al*., 2007). After incubation with the relevant secondary antibody, immunoreactive proteins were detected by luminol-enhanced chemiluminescence (Pierce). For nonreducing SDS–PAGE analyses, the abundance of SCO1 species containing oxidized disulfides and reduced thiols was quantified densitometrically for multiple exposures within the linear range of the film using ImageQuant software (Leary *et al*., 2009).

Elemental analyses

Tissue samples and cell pellets were digested in 40% nitric acid by boiling for 1 h in capped, acid-washed tubes, diluted in ultrapure, metal-free water, and analyzed by either inductively coupled plasma optical emission spectrometry (ICP-OES; Optima 3100XL; PerkinElmer, Waltham, MA) or ICP mass spectrometry (ICP-MS) versus acid-washed blanks. Concentrations were determined from a standard curve constructed with serial dilutions of two commercially available mixed metal standards (Optima). Blanks of nitric acid with and without "metal spikes" were analyzed to ensure reproducibility.

Miscellaneous

Protein concentration and COX and citrate synthase activities were measured as previously described (Leary *et al*., 2004). Statistical analyses were conducted using Prism 6 software (GraphPad, La Jolla, CA) and are detailed wherever appropriate in the figure legends.

ACKNOWLEDGMENTS

We acknowledge all of the patients and their families without whom this study would not have been possible. We thank M. Petris (University of Missouri, Columbia, MO) for the Me32 cell line and C. Duckett (University of Michigan, Ann Arbor, MI) and B. Eipper (University of Connecticut, Farmington, CT), respectively, for the COMMD1 and

ATP7A antisera. Helpful discussions with B. J. Battersby (University of Helsinki, Helsinki, Finland) and T. Wai (University of Munich, Munich, Germany) and expert technical assistance from T. Johns (Montreal Neurological Institute, McGill University, Montreal, Canada) and S. Stewart (University of Saskatchewan, Saskatoon, Canada) were invaluable to the advancement of this research. This study was supported by grants in aid of research from the Saskatchewan Health Research Foundation (S.C.L.), the Canadian Institutes of Health Research (E.A.S., S.C.L.), and the U.S. Muscular Dystrophy Association (E.A.S., S.C.L.). S.C.L. is a New Investigator of the Canadian Institutes of Health Research.

REFERENCES

Andruzzi L, Nakano M, Nilges MJ, Blackburn NJ (2005). Spectroscopic studies of metal binding and metal selectivity in *Bacillus subtilis* BSco, a homologue of the yeast mitochondrial protein Sco1p. J Am Chem Soc 127, 16548–16558.

Antonicka H, Leary SC, Guercin GH, Agar JN, Horvath R, Kennaway NG, Harding CO, Jaksch M, Shoubridge EA (2003a). Mutations in COX10 result in a defect in mitochondrial heme A biosynthesis and account for multiple, early-onset clinical phenotypes associated with isolated COX deficiency. Hum Mol Genet 12, 2693–2702.

Antonicka H, Mattman A, Carlson CG, Glerum DM, Hoffbuhr KC, Leary SC, Kennaway NG, Shoubridge EA (2003b). Mutations in COX15 produce a defect in the mitochondrial heme biosynthetic pathway, causing early-onset fatal hypertrophic cardiomyopathy. Am J Hum Genet 72, 101–114.

Balatri E, Banci L, Bertini I, Cantini F, Ciofi-Baffoni S (2003). Solution structure of Sco1: a thioredoxin-like protein Involved in cytochrome c oxidase assembly. Structure 11, 1431–1443.

Banci L, Bertini I, Calderone V, Ciofi-Baffoni S, Mangani S, Martinelli M, Palumaa P, Wang S (2006a). A hint for the function of human Sco1 from different structures. Proc Natl Acad Sci USA 103, 8595–8600.

Banci L, Bertini I, Cantini F, Felli IC, Gonnelli L, Hadjiliadis N, Pierattelli R, Rosato A, Voulgaris P (2006b). The Atx1-Ccc2 complex is a metal-mediated protein-protein interaction. Nat Chem Biol 2, 367–368.

Banci L, Bertini I, Ciofi-Baffoni S, Leontari I, Martinelli M, Palumaa P, Sillard R, Wang S (2007). Human Sco1 functional studies and pathological implications of the P174L mutant. Proc Natl Acad Sci USA 104, 15–20.

Barros MH, Johnson A, Tzagoloff A (2004). COX23, a homologue of COX17, is required for cytochrome oxidase assembly. J Biol Chem 279, 31943–31947.

Camakaris J, Danks DM, Ackland L, Cartwright E, Borger P, Cotton RG (1980). Altered copper metabolism in cultured cells from human Menkes' syndrome and mottled mouse mutants. Biochem Genet 18, 117–131.

Cobine PA, Ojeda LD, Rigby KM, Winge DR (2004). Yeast contain a non-proteinaceous pool of copper in the mitochondrial matrix. J Biol Chem 279, 14447–14455.

Cobine PA, Pierrel F, Leary SC, Sasarman F, Horng YC, Shoubridge EA, Winge DR (2006). The P174L mutation in human Sco1 severely compromises Cox17-dependent metallation but does not impair copper binding. J Biol Chem 281, 12270–12276.

Dodani SC, Leary SC, Cobine PA, Winge DR, Chang CJ (2011). A targetable fluorescent sensor reveals that copper-deficient SCO1 and SCO2 patient cells prioritize mitochondrial copper homeostasis. J Am Chem Soc 133, 8606–8616.

Glerum DM, Shtanko A, Tzagoloff A (1996). Characterization of COX17, a yeast gene involved in copper metabolism and assembly of cytochrome oxidase. J Biol Chem 271, 14504–14509.

Hamza I, Prohaska J, Gitlin JD (2003). Essential role for Atox1 in the copper-mediated intracellular trafficking of the Menkes ATPase. Proc Natl Acad Sci USA 100, 1215–1220.

Horn D, Barrientos A (2008). Mitochondrial copper metabolism and delivery to cytochrome c oxidase. IUBMB Life 60, 421–429.

Horn N (1976). Copper incorporation studies on cultured cells for prenatal diagnosis of Menkes' disease. Lancet 1, 1156–1158.

Horng YC, Leary SC, Cobine PA, Young FB, George GN, Shoubridge EA, Winge DR (2005). Human Sco1 and Sco2 function as copper-binding proteins. J Biol Chem 280, 34113–34122.

Huigsloot M, Nijtmans LG, Szklarczyk R, Baars MJ, van den Brand MA, Hendriksfranssen MG, van den Heuvel LP, Smeitink JA, Huynen MA, Rodenburg RJ (2011). A mutation in C2orf64 causes impaired cytochrome c oxidase assembly and mitochondrial cardiomyopathy. Am J Hum Genet 88, 488–493.

Jaksch M *et al*. (2001a). Homozygosity (E140K) in SCO2 causes delayed infantile onset of cardiomyopathy and neuropathy. Neurology 57, 1440–1446.

Jaksch M, Ogilvie I, Yao J, Kortenhaus G, Bresser HG, Gerbitz KD, Shoubridge EA (2000). Mutations in SCO2 are associated with a distinct form of hypertrophic cardiomyopathy and cytochrome c oxidase deficiency. Hum Mol Genet 9, 795–801.

Jaksch M *et al*. (2001b). Cytochrome c oxidase deficiency due to mutations in SCO2, encoding a mitochondrial copper-binding protein, is rescued by copper in human myoblasts. Hum Mol Genet 10, 3025–3035.

Kim BE, Nevitt T, Thiele DJ (2008). Mechanisms for copper acquisition, distribution and regulation. Nat Chem Biol 4, 176–185.

Kim BE, Turski ML, Nose Y, Casad M, Rockman HA, Thiele DJ (2010). Cardiac copper deficiency activates a systemic signaling mechanism that communicates with the copper acquisition and storage organs. Cell Metab 11, 353–363.

Lamb AL, Torres AS, O'Halloran TV, Rosenzweig AC (2001). Heterodimeric structure of superoxide dismutase in complex with its metallochaperone. Nat Struct Biol 8, 751–755.

Leary SC (2010). Redox regulation of SCO protein function: controlling copper at a mitochondrial crossroad. Antioxid Redox Signal 13, 1403–1416.

Leary SC *et al*. (2007). The human cytochrome c oxidase assembly factors SCO1 and SCO2 have regulatory roles in the maintenance of cellular copper homeostasis. Cell Metab 5, 9–20.

Leary SC, Kaufman BA, Pellecchia G, Guercin GH, Mattman A, Jaksch M, Shoubridge EA (2004). Human SCO1 and SCO2 have independent, cooperative functions in copper delivery to cytochrome c oxidase. Hum Mol Genet 13, 1839–1848.

Leary SC, Sasarman F, Nishimura T, Shoubridge EA (2009). Human SCO2 is required for the synthesis of CO II and as a thiol-disulphide oxidoreductase for SCO1. Hum Mol Genet 18, 2230–2240.

Lee J, Pena MM, Nose Y, Thiele DJ (2002). Biochemical characterization of the human copper transporter Ctr1. J Biol Chem 277, 4380–4387.

Longen S, Bien M, Bihlmaier K, Kloeppel C, Kauff F, Hammermeister M, Westermann B, Herrmann JM, Riemer J (2009). Systematic analysis of the twin cx(9)c protein family. J Mol Biol 393, 356–368.

Lutsenko S, Barnes NL, Bartee MY, Dmitriev OY (2007). Function and regulation of human copper-transporting ATPases. Physiol Rev 87, 1011–1046.

Moffat J *et al*. (2006). A lentiviral RNAi library for human and mouse genes applied to an arrayed viral high-content screen. Cell 124, 1283–1298.

Nobrega MP, Bandeira SC, Beers J, Tzagoloff A (2002). Characterization of COX19, a widely distributed gene required for expression of mitochondrial cytochrome oxidase. J Biol Chem 277, 40206–40211.

Papadopoulou LC *et al*. (1999). Fatal infantile cardioencephalomyopathy with COX deficiency and mutations in SCO2, a COX assembly gene. Nat Genet 23, 333–337.

Pase L, Voskoboinik I, Greenough M, Camakaris J (2004). Copper stimulates trafficking of a distinct pool of the Menkes copper ATPase (ATP7A) to the plasma membrane and diverts it into a rapid recycling pool. Biochem J 378, 1031–1037.

Pear WS, Nolan GP, Scott ML, Baltimore D (1993). Production of high-titer helper-free retroviruses by transient transfection. Proc Natl Acad Sci USA 90, 8392–8396.

Petris MJ, Mercer JF (1999). The Menkes protein (ATP7A; MNK) cycles via the plasma membrane both in basal and elevated extracellular copper using a C-terminal di-leucine endocytic signal. Hum Mol Genet 8, 2107–2115.

Petris MJ, Strausak D, Mercer JF (2000). The Menkes copper transporter is required for the activation of tyrosinase. Hum Mol Genet 9, 2845–2851.

Rae TD, Schmidt PJ, Pufahl RA, Culotta VC, O'Halloran TV (1999). Undetectable intracellular free copper: the requirement of a copper chaperone for superoxide dismutase. Science 284, 805–808.

Steenaart NA, Shore GC (1997). Mitochondrial cytochrome c oxidase subunit IV is phosphorylated by an endogenous kinase. FEBS Lett 415, 294–298.

Stiburek L, Vesela K, Hansikova H, Hulkova H, Zeman J (2009). Loss of function of Sco1 and its interaction with cytochrome c oxidase. Am J Physiol Cell Physiol 296, C1218–C1226.

Valnot I, Osmond S, Gigarel N, Mehaye B, Amiel J, Cormier-Daire V, Munnich A, Bonnefont JP, Rustin P, Rotig A (2000). Mutations of the SCO1 gene in mitochondrial cytochrome c oxidase deficiency with neonatal-onset hepatic failure and encephalopathy. Am J Hum Genet 67, 1104–1109.

Williams JC, Sue C, Banting GS, Yang H, Glerum DM, Hendrickson WA, Schon EA (2005). Crystal structure of human SCO1: implications for redox signaling by a mitochondrial cytochrome c oxidase "assembly" protein. J Biol Chem 280, 15202–15211.